CHARACTERISTICS OF SMOKE CONCENTRATION PROFILES WITH UNDERGROUND UTILITY TUNNEL FIRE

Hong-Sik Kim[1], In-Ju Hwang[2] and Youn-Jea Kim[3*]

Accurate prediction of the fire-induced air velocity, temperature and smoke flow in underground utility tunnel becomes more important for the optimization of design and placement of heat and smoke detectors. In order to improve the safety of underground utility tunnel systems, the behaviors of fire-induced smoke flow and temperature distributions are investigated. Especially, two different cross-sectional shapes of tunnel, such as rectangular and circular types are modeled. Also, fire source is modeled as a volumetric heat source. Three-dimensional thermal-flow characteristics in an underground tunnel are solved by means of FVM using SIMPLE algorithm. The effects of shape geometry on the fire-induced flow characteristics are graphically depicted. It is desirable that heat and smoke detectors are installed on the cables and the top of the wall.

Keywords: Temperature Distribution, Smoke Flow, Volumetric Heat Source(VHS) Model, Underground Utility Tunnel Systems

1. INTRODUCTION

The underground utility tunnel systems mainly contain communication and electric power cables. Numerous fires occurred in grouped cables, because the plastics used for cable insulation and jacketing materials are combustible. Cable fires may be started by any number of ignition sources, such as electrical arcing, exposure to fire from other combustibles, and cutting and welding, etc.

If a fire breaks out in this underground utility tunnel, the fire spreads over the cable surface, accompanied by the generation of heat and smoke. Heat from fire involving cables can create a hazardous thermal environment. Generation of smoke and toxic products may create a hazardous non-thermal environment. Consequently, the function of the city will be discontinued and be resulted in huge damages. Therefore, accurate prediction of the fire-induced flow velocity, temperature and smoke concentration in utility tunnel becomes more important for designing of the efficient fire protection and prevention systems.

Many investigators studied the fire simulation that deals with the development of the descriptions of the fire phenomena. Especially, they described physical and chemical processes as functions of the ignition source, space geometry and material contents. Baum et al.[1] reviewed computations designed to predict the evolution of the size distribution of smoke aerosol as it ages, as well as the large-scale air movement and temperature fields generated by an enclosure fire. An approach to field modeling of fire phenomena in enclosures is also presented by McGrattan et al.[2] They calculated the conservation equations of mass, momentum and energy with sufficient temporal and spatial resolution to yield a truly three-dimensional, dynamic picture of the fire plume and its surroundings. Woodburn and Britter[3] performed the simulations of the area around the fire. In the fire area simulations, the upstream smoke layer length was found to be sensitive to the ventilation velocity profile, the turbulence model used and the heat input rate. Lea[4] used three computational models to study the effects of fire in an UK mine by employing one-dimensional gravity current techniques of measuring stratified flow up to breakdown.

Received: July 19, 2004, Accepted: March 7, 2005.
1 Graduate School of Mechanical Engineering, Sung-kyunkwan University, 300 Cheoncheon-dong, Suwon 400-746, Korea
2 Korea Institute of Construction Technology
3 School of Mechanical Engineering, Sungkyunkwan University, 300 Cheoncheon-dong, Suwon 400-746, Korea
* Corresponding author. E-mail: yjkim@skku.edu

The aim of present study is to investigate the effects of space geometry on the fire-induced flow fields in underground utility tunnel systems (see Fig. 1). Therefore, an understanding of this prediction is important for the optimization of design and placement of heat and smoke detectors.

2. FORMULATION OF THE PROBLEM

Heated air movement is the key concern in an underground utility tunnel. The turbulent buoyant flow is governed by the equations expressing the conservation of mass, momentum energy and concentration of species. When the unsteady-state process is considered, the governing equations can be written in a Cartesian tensor form as follows:

continuity:

$$\frac{\partial \rho}{\partial t}+\frac{\partial}{\partial x_i}(\rho u_i)=0 \tag{1}$$

momentum:

$$\frac{\partial \rho u_i}{\partial t}+\frac{\partial}{\partial x_j}(\rho u_j u_i)=-\frac{\partial p}{\partial x_i}+\frac{\partial \tau_{ij}}{\partial x_j} \tag{2}$$

turbulent kinetic energy equation:

$$\frac{\partial \rho k}{\partial t}+\frac{\partial}{\partial x_j}(\rho u_j k) =\frac{\partial}{\partial x_j}(\mu+\frac{\mu_t}{\sigma_k})\frac{\partial k}{\partial x_j}+G-\rho\varepsilon \tag{3}$$

turbulent kinetic energy dissipation equation:

$$\frac{\partial \rho \varepsilon}{\partial t}+\frac{\partial}{\partial x_j}(\rho u_j \varepsilon) =\frac{\partial}{\partial x_j}(\mu+\frac{\mu_t}{\sigma\varepsilon})\frac{\partial \varepsilon}{\partial x_j}+\frac{\varepsilon}{k}(C_1 G-C_2\rho\varepsilon) -\frac{C_\mu \eta^3(1-\eta/\eta_0)}{1+\beta\eta^3}\cdot\frac{\rho\varepsilon^2}{k} \tag{4}$$

Table. 1 Boundary and Initial Conditions

Left	Symmetry
Right	Opening(Neumann)
Wall	No-slip, Adiabatic
Cables	Adiabatic
Heat source	VHS(4.2 MW)
Initial Temp.	19℃

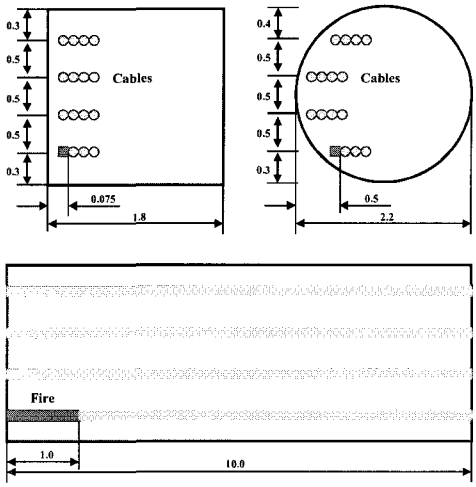

Fig. 1 Schematic diagram of the utility tunnel systems (unit: m) (top: cross-sectional view of rectangular and circular tunnels; bottom: longitudinal view).

concentration equation:

$$\frac{\partial}{\partial x_j}(\rho u_j C_s)=\frac{\partial}{\partial x_j}(\mu+\frac{\mu_t}{S_c})\frac{\partial C_s}{\partial x_j} \tag{5}$$

where,

$$\tau_{ij}=-(\mu+\mu_t)(\frac{\partial u_i}{\partial x}+\frac{\partial u_j}{\partial x_i})-\frac{2}{3}\rho k\delta_{ij},$$
$$\mu_t=C_\mu\rho\frac{k^2}{\varepsilon}, G=2\mu_t S_{ij}\frac{\partial u_i}{\partial x_j}, \eta=S\frac{\varepsilon}{k}, \tag{6}$$
$$S_{ij}=\frac{1}{2}\mu_t(\frac{\partial u_i}{\partial x_j}+\frac{\partial u_j}{\partial x_i}), S=\sqrt{(2S_{ij}S_{ij})}$$

Here C_s denotes the magnitude of concentration (less than 1.0), S_c the Schmidt number(equal to 1.0), C_μ=0.085, C_1=1.42, C_2=1.68, C_3=0.085, σ_k=0.719, σ_ε=0.719, η_0=4.38 and β=0.012. For the closure of the governing equations, the standard $k-\varepsilon$ model of turbulence is used.[5]

In order to represent the combustion behaviors, the volumetric heat source (VHS), the eddy break-up and the presumed probability density function (pre-PDF) models are generally used. First, the VHS model does not take into account for chemical reactions, instead, it sets the heat release rate equivalent to that of the assumed fire. This is the simplest fire model and easy for implementation.[6] In this study, we used this VHS model. The second

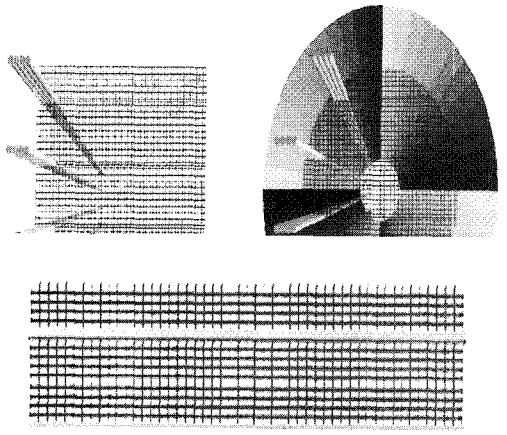

Fig. 2 Computational grid systems of the underground utility tunnel (50×50×100 cells).

is the eddy break-up model presented by Magnussen and Hjertager[7], which is simultaneously taken into accounted for mixing and finite chemical reaction rates. The third is a mixture fraction approach using pre-PDF model, where an assumed PDF shape is generally used to take into account for turbulence-chemistry interaction.

Simulation of the fire-induced flow fields in the underground utility tunnel was carried out with 50×50×100 cells, as shown in Fig. 2. In the present work the ignition point was located at the inlet side of the underground utility tunnel and assumed its heat release rate of 4.2 MW. In addition, we assumed that the heat source is uniformly distributed in a volume of 0.05 m×0.05 m×1.0 m.

Table 1 shows the boundary and initial conditions. No-slip condition is used on the wall boundary. This is presumed that there is no mass flux on walls. In order to reduce a number of cells, the wall function was used. In addition, Neumann condition that has zero gradient for all flow variables along streamline was selected on the outlet boundary, since the flow variables were difficult to know on the outlet boundary. The adiabatic condition was also used on the cables.

The change of length of model from 20 m to 200 m(location of ventilation hole) does not affect the solutions significantly because of no friction and adiabatic condition at wall. Therefore, the length of utility tunnel model was set to 20 m.

Fig. 3 shows the temperature measurement points which are located on the center of ceiling for the

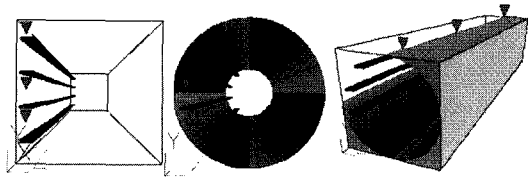

Fig. 3 Temperature measurement points(▼) of the underground utility tunnel.

horizontal direction(X=0.3, 0.5, 0.9) and on the wall for the vertical direction(Y=0.3, 0.5, 1.0) in the underground utility tunnel.

3. SOLUTION METHOD

The governing equations are solved by the finite volume method with staggered grid systems, using PHOENICS[5], a commercial computational fluid dynamics (CFD) code. The SIMPLE (Semi-Implicit Method for Pressure-Linked Equations) algorithm and hybrid scheme are also employed.

As the convergence criterion, the sum of the normalized absolute residuals in each control volume for all variables is controlled to be less than 10^{-4} and the change of number of grid points above about 250,000 does not affect the solutions significantly.

4. RESULTS AND DISCUSSION

Fig. 4 shows the temperature profiles along the vertical direction (Y-direction) of the rectangular and cylindrical tunnels. It was analyzed during 180 seconds and the origin of fire was located at the first shelf of the cables, the lowest one. The distribution of temperature is plotted each 30 seconds. Firstly, for the case of a rectangular type, it is seen that the temperatures rise up to 105°C after 30 seconds at the point (Y=0.3). Rising continuously after that time, it reaches up to 160°C at 3 minutes after ignition. At the end of vertical direction (Y=0.9), the temperature increases at time transit. However, the temperature is rapidly decreased along the vertical direction of the underground utility tunnel (approximately, ΔT =58°C after 180 s). It is also seen that the hot gas is widely dispersed to the ceiling.

In the case of a cylindrical type, the maximum temperature is approximately 100°C, and it is lower

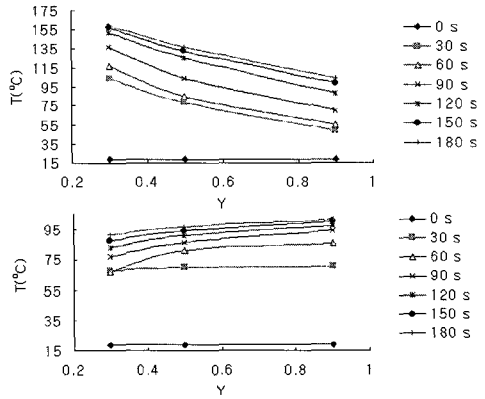

Fig. 4 Temperature variations along the vertical wall(top: rectangular, bottom: circular).

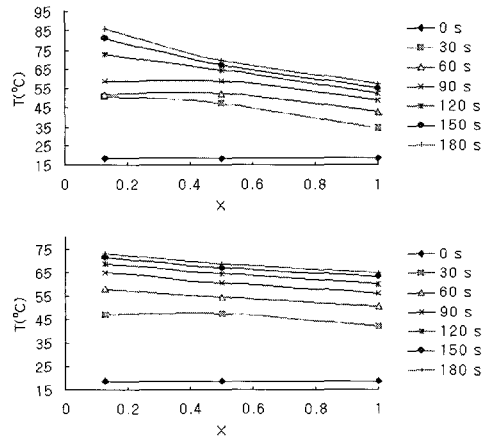

Fig. 5 Temperature variations on the ceiling along the horizontal direction(top: rectangular, bottom: circular).

than that of the rectangular one. However, the temperature is increased along the vertical wall. This is because the hot gas concentrates on the top of ceiling for the cylindrical type.

Temperature variations on the ceiling of the rectangular and cylindrical tunnels along the horizontal direction (X-direction) are shown in Fig. 5. For the case of a rectangular type, although the initial temperature is 19°C, the temperature near the heat source rises to 50°C at 30 seconds after ignition. Though the rate of temperature rise decreased at time transit, the temperature was increased to 90°C at 3 minutes after ignition. However, the temperature is rapidly decreased along the horizontal direction of the underground

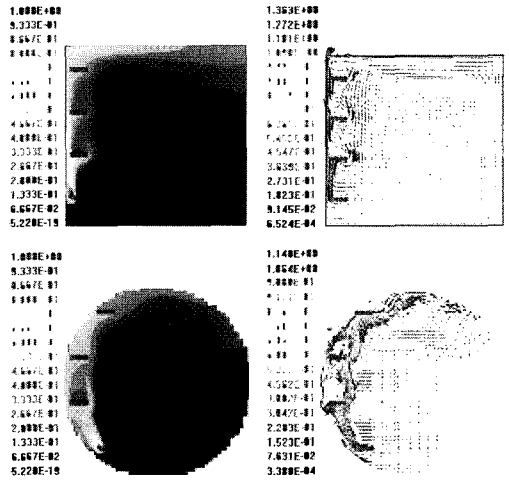

Fig. 6 Distributions of smoke and velocity vector in vertical cross-section (center of heat source) at 180 seconds after ignition.

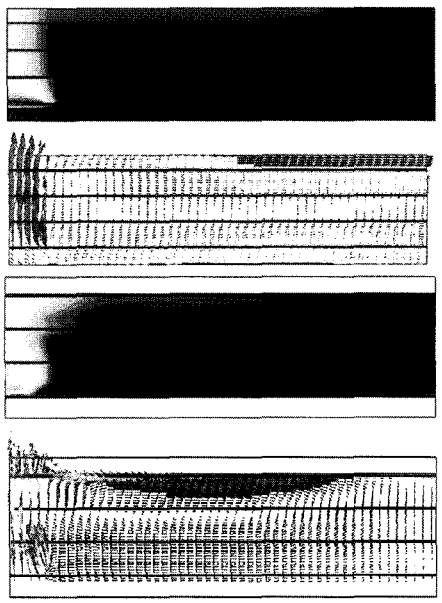

Fig. 7 Distributions of smoke and velocity vector in horizontal cross-section at 180 seconds after ignition(the legend is equal to Fig. 6).

utility tunnel (nearly, ΔT =28°C after 180 s). It is considered that the hot gas is widely distributed on the ceiling by the effect of geometrical shape and it rapidly flows out to the exit.

For the case of a cylindrical type, the distributions of temperature along the horizontal

direction show alike. However, the maximum temperature (74°C) of cylindrical type is lower than that of the rectangular one. Results also show that the temperature is almost unchanged along the horizontal direction of the underground utility tunnel (nearly, ΔT =7°C after 180 s). It is seen that the hot air-stream is distributed at the center of ceiling and does not rapidly flow out to the exit.

It is judged that temperature is smaller as compared with calorific value because heat source volume is small even though fire strength is big.

Fig. 6 shows the distribution of smoke and velocity vector in vertical cross-section of rectangular and cylindrical tunnels at 180 seconds after ignition. It is seen that the smoke mainly is raised along the wall. Also the location of rapid (1.3 m/s) hot gas appears over the 2-stage cable in the vicinity of the wall. In addition, a small region of circulation is appeared over the cables for the case of a rectangular tunnel. However, it does not appear in the vicinity of ceiling. Also, in the case of cylindrical type, the region of circulation is appeared over the cables and developed to the ceiling. The location of rapid (1.1 m/s) hot gas is far from the wall and over the 2-stage cable.

Fig. 7 shows the distribution of smoke and velocity vector in the horizontal cross-section of rectangular and cylindrical tunnels at 180 seconds later. For the case of a rectangular type, it is seen that the smoke above heat source constantly rises and mainly flows out to the exit. It is also seen that the streamlines are mainly formed from heat source to the exit at the ceiling of underground utility tunnel.

For the case of cylindrical type, however, the distribution of smoke is more complicated than that of rectangular one. Especially, the smoke is formed thickly at the center of ceiling and does not quickly flow out to the exit. That is because of opening condition at the outlet and a small magnitude of the heat source as well as geometry. Furthermore, streamlines are formed from the exit to the heat source at the bottom of utility tunnel. It is also noted that the circulation is formed at the center of underground utility tunnel.

5. CONCLUSIONS

In this study, we have investigated the fire-induced flow characteristics in the underground utility tunnel with two different cross-sectional shapes. Especially, volumetric heat source (VHS) model is used to describe the fire source. And the effects of geometrical shapes on the profiles of temperature and smoke flow are depicted. In the case of a cylindrical type, the maximum temperature is approximately 100C°, and it is lower than that of the rectangular one. It is desirable that heat and smoke detectors are installed on the cables and the top of the wall because the smoke and hot gas mainly move along the wall and the cables. In the case of a cylindrical type, the maximum temperature is approximately 100C°, and it is lower than that of the rectangular one.

ACKNOWLEDGEMENT

The authors are grateful for the financial support provided by the Ministry of Construction & Transportation through the Korea Institute of Construction Technology (E-01).

REFERENCES

[1] Baum, H.R., Rehm, R.G. and Mulholland, G.W., 1983, "Prediction of heat and smoke movement in enclosure fires," *Fire Safety J.*, Vol.6, pp.193-201.

[2] McGrattan, K.B., Baum, H.R. and Rehm, R.G., 1998, "Large eddy simulations of smoke movement," *Fire Safety J.*, Vol.30, pp.161-178.

[3] Woodburn, P.J. and Britter, R.E., 1996, "CFD simulation of a tunnel fire-Part I," *Fire Safety Journal*, Vol.26, pp.35-62.

[4] Lea, C.J., 1994, "Computational modeling of mine fires," *Mine Eng.*(London), Vol.154(394), pp.17-21.

[5] PHOENICS, Ver. 3.4, 2001, *User Manual*, Advanced Computational Technology for Engineering.

[6] Xue, H., Ho, J.C., and Cheng, Y.M., 2001, "Comparison of different combustion models in enclosure fire simulation," *Fire Safety Journal*, Vol.36, pp.37-54.

[7] Magnussen, B.F. and Hjertager, B.H., 1976, "On mathematical models of turbulent combustion with special emphasis on soot formation and combustion," *16th Int. Symposium on Combustion*, pp.719-729.